Experimental study on torque and burrs during ultrasonic assisted single-pass honing of 4Cr13 stainless steel

Shaowu Gao*, Changyong Yang, Jiuhua Xu

College of Mechanical and Electrical Engineering, Nanjing University of Aeronautics and Astronautics, Nanjing, 210016, China

E-mail: shwgao@163.com

Keywords: Ultrasonic, single-pass honing, torque, burr, honing speed, feed per revolution.

Abstract. Combining the advantages of single-pass honing and ultrasonic machining, ultrasonic assisted single-pass honing (UASH) have great potential in high efficiency manufacturing of valves. In this paper, a series of honing experiments were carried out on 4Cr13 martensitic stainless steel. The peak value and mean value of torque during honing were measured. Besides, the burrs of the entrance and exit of honed holes were observed. The results showed that torque of UASH is much smaller than the one of conventional single-pass honing (CSH), under the same honing parameters. Within the honing parameters adopted, the effect of honing speed on torque is not significant. With the increase of hole length and feed per revolution, both peak value and mean value of the torque increase significantly. From the point of view of torque, compared with CSH, UASH is more suitable for high efficiency machining. The observations of burrs showed that the burrs shape randomly at the entrance and exit. And the burrs produced in single-pass honing can be classified as no apparent burrs, warping burrs, crimped burrs and adhesive burrs.

Introduction

As honing can obtain holes with good form accuracy as well as good surface roughness, it is one of the best alternatives as the finishing technology in manufacturing high precision valves [1-3]. However, the stiffness of honing machine is weak due to the slender structure of feeding system [4]. The variation in diameter and surface roughness of bores before honing can be easily inherited into the honed parts, resulting in inconsistency of honed diameter [5].

Different with conventional honing, single-pass honing is generally carried out with fixed-size honing tools. Therefore, compared with conventional honing, single-pass honing can obtain holes with tight tolerance [6]. Due to this feature, single-pass honing has great potential in manufacturing of holes with high consistency.

However, the workpiece and honing tool are surface contact during single-pass honing. The effects of coolant and chip removal in contact area are poor. This shortcoming limits the material removal rate during single-pass honing of ductile materials.

Due to the benefits on cavitation and chip breaking of ultrasonic vibration, comparing with traditional machining, ultrasonic assisted machining can reduce cutting force and improving machining efficiency [7-9]. Therefore, ultrasonic assisted machining is widely used in abrasive manufacturing process, such as grinding and honing [10-13]. Similarly, the advantages of ultrasonic assisted single-pass honing (UASH) is also predictable. Nevertheless, few papers have been published on the process characteristics of UASH.

In this paper, several single-pass honing experiments were carried out to study the influence of honing parameters, including feed rate, ultrasonic vibration, etc. on honing torques. Besides,

considering the importance of burrs to the performance of honed parts [14], burrs after honing were observed to help the optimization of honing parameters.

Experimental setup and conditions

The experimental setup is shown in Fig. 1. The honing experiments were conducted on DMG Ultrasonic 20 Linear Machining Center. Castrol Syntilo 9954 was used as the coolant and the concentration was 5% (mass). Electroplated CBN honing tool were utilized in honing tests. The diameter of CBN grains ranged from 125μm to 150μm. The frequency of ultrasonic vibration of honing tool was set at 22600Hz. And the amplitude of tool end was close to 5μm. Workpiece material is 4Cr13 martensitic stainless steel, and the hardness is over 50HRC after quenching. The holes were reamed into diameters between 4.028mm and 4.030mm. The workpiece was clamped by a floating fixture and the floating gap was set at 0.2mm. Honing parameters used in the experiments were shown in Table 1.

Kistler 9272 dynamometer was utilized to measure the torque during honing. The typical torque signal is shown in Fig. 2. It can be seen that the single-pass honing process contains three stages: cut-in, polishing and retraction. At each stage, the torque signal has different features. Both peak value and average value were utilized to evaluate the torque during honing.

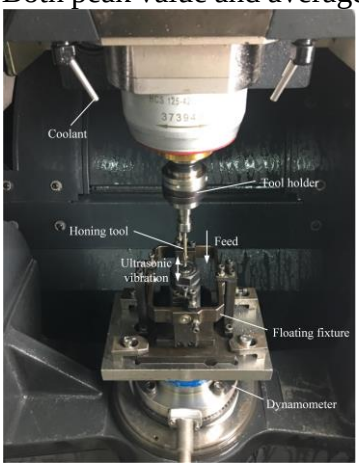

Fig. 1 Experimental setup

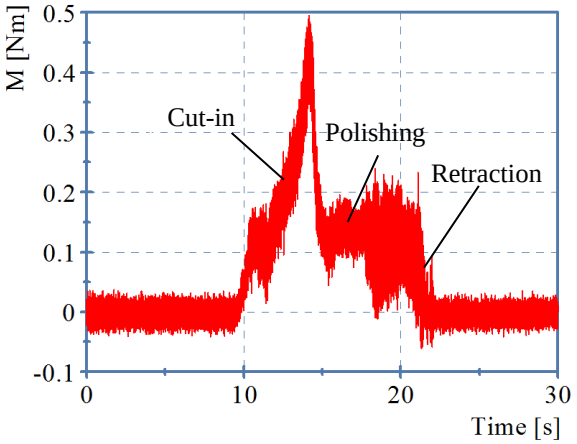

Fig. 2 Typical signal of honing torque (*n*=2000r/min, va=75mm/min, CSH)

Table 1 Honing parameters

Factors	Values
Tool rotating speed *n* (r/min)	1000, 2000, 3000
Feed per revolution *f* (μm/r)	12.5, 17.5, 25, 37.5, 40, 50, 62.5
Ultrasonic vibration	Yes/No
Hole length *L* (mm)	4, 6, 8

The topographies of burrs after honing were observed with SENSOFAR 3-D optical surface profiler. The measured 3-D topography of burr was shown in Fig. 3. In order to see curling burrs clearly, workpiece after honing was split along the axis and the cross-sectional topographies of burrs were observed with Leica Metallographic Microscope, as shown in Fig. 4.

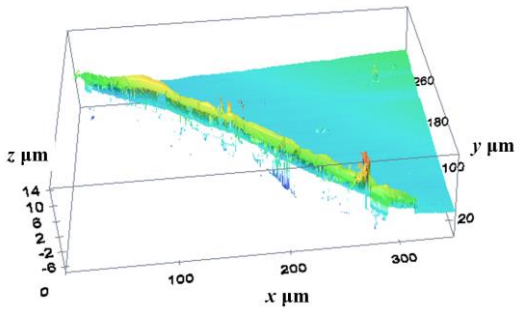

Fig. 3 3-D topography of burr

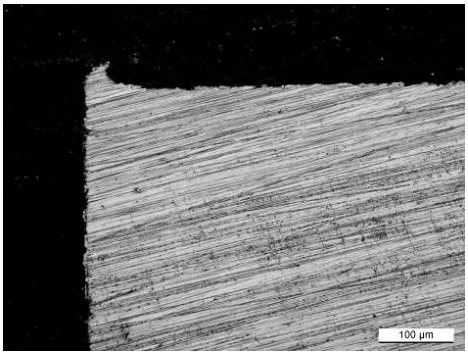

Fig. 4 Cross-sectional topography of burr

Results and analysis

Honing torques with different tool rotating speeds, under f=40µm/r, L=4mm, were shown in Fig. 5. It can be seen that the value of average torque reduces from 0.1358N·m to 0.093N·m with the increase of tool rotating speed from 1000r/min to 3000r/min. It may be caused by the thermal soften effect of workpiece material during honing. Heat flux density increased with the increase of honing speed, resulting in higher honing temperature. The softening of the workpiece material caused the reduction of cutting force and honing torque.

Besides, both average and peak torques of UASH are much smaller than the ones of CSH, especially at low tool rotating speeds. Fig. 6 shows the cutting trajectory of single grit during single-pass honing, including CSH and UASH. It can be seen that, under same honing parameters, cutting trajectory in UASH is longer than the one in CSH [15]. The increase of cutting path can decrease the cutting thickness of single grit, reducing the cutting force and torque. Keep the parameter of ultrasonic vibration constant, the length of cutting path increases significantly at lower honing speed. Therefore, the effect of ultrasonic vibration is more significant at lower honing speed.

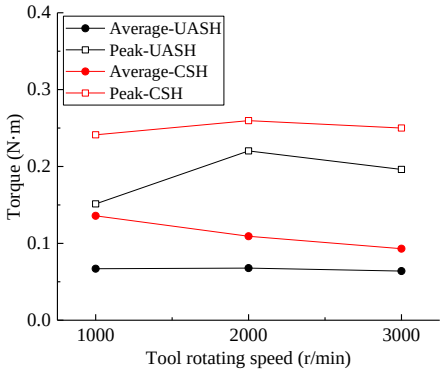

Fig. 5 Honing torque vs tool rotating speed (f=40µm/r, L=4mm)

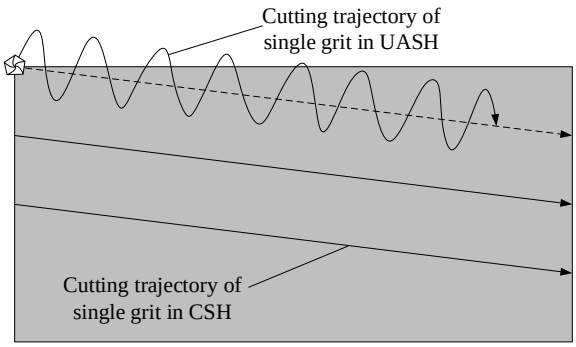

Fig. 6 Diagram of cutting trajectory of single grit

The honing torques with different feeding speeds, under n=2000r/min, L=4mm, are shown in Fig. 7. It can be seen that average torque and peak torque of CSH respectively increase from 0.08195N·m to 0.1426N·m and from 0.139N·m to 0.4197N·m, when feed per revolution increase from 12.5µm/r to 37.5µm/r. Besides, when feed per revolution increase from 12.5µm/r to 62.5µm/r, average torque and peak torque of UASH respectively increase from 0.02112N·m to 0.1168N·m and from 0.0332N·m to 0.4248N·m. It can be concluded that feed per revolution has great influence on honing torque. And with the increase of feed per revolution, honing torque increase rapidly, especially the peak value of honing torque. In addition, with same

honing torque, the maximum material removal rate of UASH is much larger than the one of CSH.

Fig. 8 shows the specific energy of CSH under different feed per revolution. Increasing feed per revolution from 12.5μm/r to 37.5μm/r, the specific energy reduces from 1908.32J/mm^3 to 1261.26J/mm^3. The reason is that the cutting thickness of single grit increases with the increase of feed per revolution, resulting in the reduction of specific energy.

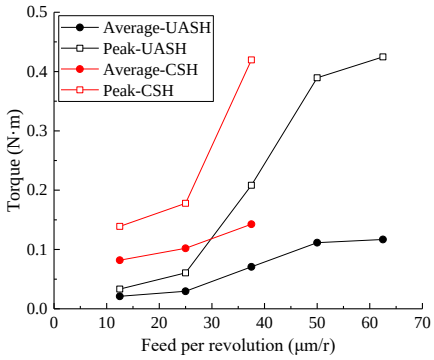

Fig. 7 Honing torque vs. feeding speed (n=2000r/min, L=4mm)

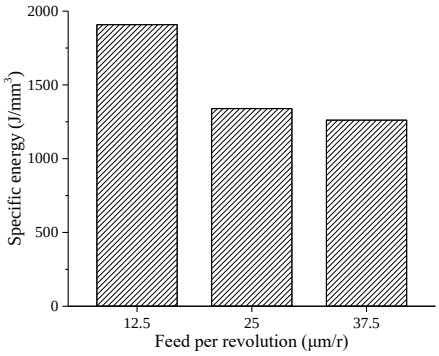

Fig. 8 Specific energy vs. feeding speed (n=2000r/min, L=4mm)

Honing torques with different hole lengths, under n=2000r/min, f=17.5μm/r, are shown in Fig. 9. It can be seen that, under the same honing parameters, honing of long holes accompanies with larger honing torques. Due to the face contact feature of single-pass honing, the contact area between workpiece and honing tool are larger when honing of longer holes, resulting in larger honing torques. By comparing CSH and UASH, it can also be concluded that the ultrasonic vibration can greatly improve the machining states of contacting region.

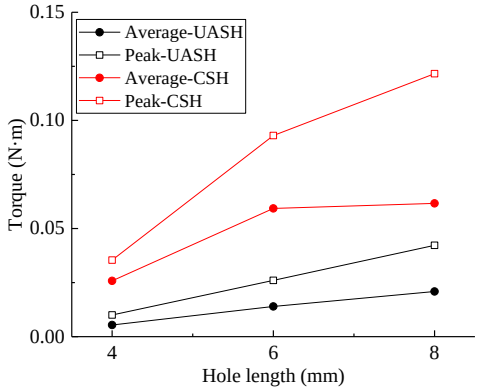

Fig. 9 Honing torque vs hole length (n=2000r/min, f=17.5μm/r)

Burrs inevitably appear in single-pass honing of ductile materials. And burrs have significant influence on the stability and reliability of honed parts. Burrs at different positions of the entrance after CSH under n=2000r/min, f=17.5μm/r, L=4mm, are shown in Fig. 10. It can be seen that the shape and size of burrs are quite different along the circumference of the same hole. It may result from the undefined cutting states at different positions caused by undefined cutting edges during honing.

(a) Measuring positions (b) 0° (c) 135° (d) 225°

Fig. 10 Burrs at different positions of the same hole (n=2000r/min, f=17.5μm/r, L=4mm, CSH, Entrance)

By observation on burrs of honed holes, burrs produced by single-pass honing can be divided into four kinds: no apparent burrs, crimped burrs, warping burrs and adhesive burrs, as shown in Fig. 11. Different kind of burrs occurred under different cutting states. Although the morphology of burrs showed randomness to a certain extent, the influence of honing parameters on burrs still follow some rules. Honing under small feed rates tends to produce crimped burrs, while honing under large feed rates tends to produce warping burrs.

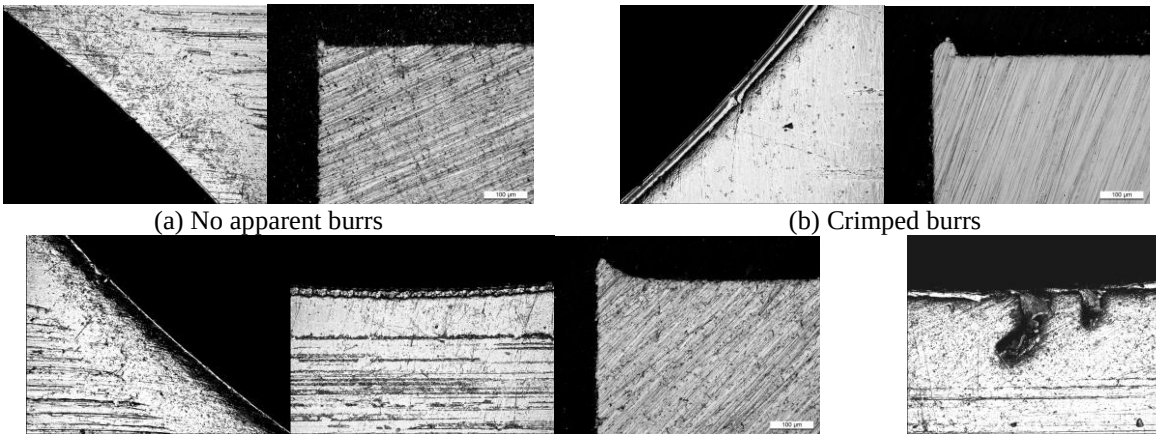

(a) No apparent burrs (b) Crimped burrs

(c) Warping burrs (d) Adhesive burrs

Fig. 11 Classification of burrs produced in single-pass honing

Conclusions

Both CSH and UASH experiments have been carried out. And the honing torque and burrs are analyzed. The results showed that ultrasonic vibration can effectively decrease honing torque and improve honing efficiency. Honing torque of both CSH and UASH increased with the increase of feed per revolution and hole length. Due to the randomness of cutting edges during honing, the burrs also showed randomness to a certain extent. And burrs produced by single-pass honing can be divided into four kinds: no apparent burrs, crimped burrs, warping burrs and adhesive burrs.

References

[1] F. Klocke, Manufacturing Processes 2: Grinding, Honing, Lapping, Springer, Berlin, 2009.

[2] W. G. Drossel, C. Hochmuth, R. Schneider, An adaptronic system to control shape and surface of liner bores during the honing process, CIRP Ann. Manuf. Technol. 62(1) (2013) 331-334.

[3] S. Gao, C. Yang, J. Xu, Y. Fu, H. Su, W. Ding, Optimization for internal traverse grinding of valves based on wheel deflection, Int. J. Adv. Manuf. Technol. 92 (2017) 1105-1112.

[4] C. Schmitt, D. Bähre, An Approach to the Calculation of Process Forces During the Precision Honing of Small Bores, Procedia CIRP. 7 (2013) 282-287.

[5] F. J. Chen, S. H. Yin, H Huang, H Ohmori, Profile error compensation in ultra-precision grinding of aspheric surfaces with on-machine measurement, Int. J. Mach. Tool Manu. 50(5), (2010) 480-486.
[6] S. Arunachalam, A. Gunasekaran, J.M. O'Sullivan, Analysing the process behaviour of abrasive reaming using an experimental approach, Int. J. Mach. Tool Manu. 39 (1999) 1311-1325.
[7] T.B. Thoe, D.K. Aspinwall, M.L.H. Wise, Review on ultrasonic machining, Int. J. Mach. Tool Manu. 38 (1998) 239-255.
[8] R. Singh, J.S. Khamba, Ultrasonic machining of titanium and its alloys: A review, J Mater Process Tech. 173 (2006) 125-135.
[9] D.E. Brehl, T.A. Dow, Review of vibration-assisted machining, Precis. Eng. 32 (2008) 153-172.
[10] J. Cao, Y. Wu, J. Li, Q. Zhang, A grinding force model for ultrasonic assisted internal grinding (UAIG) of SiC ceramics, Int. J. Adv. Manuf. Technol. 81 (2015) 875-885.
[11] M.F. Ismail, K. Yanagi, H. Isobe, Geometrical transcription of diamond electroplated tool in ultrasonic vibration assisted grinding of steel, Int. J. Mach. Tool Manu. 62 (2012) 24-31.
[12] M. Zhou, X.J. Wang, B.K.A. Ngoi, J.G.K. Gan, Brittle–ductile transition in the diamond cutting of glasses with the aid of ultrasonic vibration, J. Mater. Process Tech. 121 (2002) 243-251.
[13] Z. Bo, L. Chuanshao, G. Guofu, J. Feng, Surface characteristics in the ultrasonic ductile honing of ZrO2 ceramics using coarse grits, J. Mater. Process Tech. 123 (2002) 54-60.
[14] J.C. Aurich, D. Dornfeld, P.J. Arrazola, V. Franke, L. Leitz, S. Min, Burrs—Analysis, control and removal, CIRP Ann. Manuf. Technol. 58 (2009) 519-542.
[15] E. Bertsche, K. Ehmann, K. Malukhin, An analytical model of rotary ultrasonic milling, Int. J. Adv. Manuf. Technol. 65 (2013) 1705-1720.